Which Multi-Heme Protein Complex Transfers Electrons More Efficiently? Comparing MtrCAB from *Shewanella* with OmcS from *Geobacter*

Xiuyun Jiang[1], Jessica H. van Wonderen[2], Julea N. Butt[2], Marcus J. Edwards[2], Thomas A. Clarke[2], Jochen Blumberger[1*]

[1]Department of Physics and Astronomy and Thomas Young Centre, University College London, London WC1E 6BT, United Kingdom.
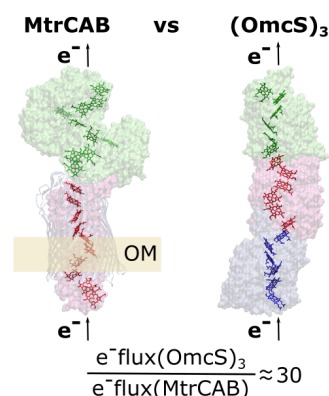[2]School of Chemistry and School of Biological Sciences, University of East Anglia, Norwich Research Park, Norwich, NR4 7TJ, United Kingdom.

Supporting Information Placeholder

ABSTRACT: Microbial nanowires are fascinating biological structures allowing bacteria to transport electrons over micrometers for reduction of extracellular substrates. It was recently established that the nanowires of both *Shewanella* and *Geobacter* are made of multi-heme proteins, but while *Shewanella* employs the 20-heme protein complex MtrCAB, *Geobacter* uses a redox polymer made of the hexa-heme protein OmcS, begging the question which protein architecture is more efficient in terms of long-range electron transfer. Using a multiscale computational approach we find that OmcS supports electron flows about an order of magnitude higher than MtrCAB due to larger heme-heme electronic couplings and better insulation of hemes from the solvent. We show that heme side chains are an essential structural element in both protein complexes accelerating rate-limiting electron tunnelling steps up to 1000-fold. Our results imply that the alternating stacked/T-shaped heme arrangement present in both protein complexes may be an evolutionarily convergent design principle permitting efficient electron transfer over very long distances.

TOC graphic:

Certain microbes have developed a fascinating strategy to respire under anaerobic conditions. They export electrons from the interior of the cell, were they accumulate due to metabolic reactions, to substrates outside the cell, e.g. solid-phase Fe(III) and Mn(III/IV) oxides. This process, termed extracellular respiration[1-2], is of global environmental significance as it contributes to the natural cycling of transition metal ions and the removal of metal pollutants, e.g. U(VI). Moreover, extracellular respiration underpins a new generation of renewable energy technologies that incorporate microbes as catalysts on electrode surfaces including microbial fuel cells and microbial electrosynthesis of fuels and chemical feedstock[2].

Shewanella employs the 20-heme protein complex MtrCAB [3-4] for electron export across the outer bacterial membrane, whereas *Geobacter* uses a redox-active protein polymer made of the hexa-heme protein OmcS [5], see Figure 1. Very recently, the atomistic structure of MtrCAB [6] and OmcS [5] have been reported begging the question which electron export strategy – protein complex or protein polymer – is more efficient. In particular, one may wonder which structure supports higher electron transfer (ET) rates in extracellular respiration. Here we calculate the maximum, i.e. protein limited, electron flux through these structures and predict that OmcS outperforms MtrCAB by about one order of magnitude due to better electronic coupling between the protein subunits and less solvent exposure of the hemes.
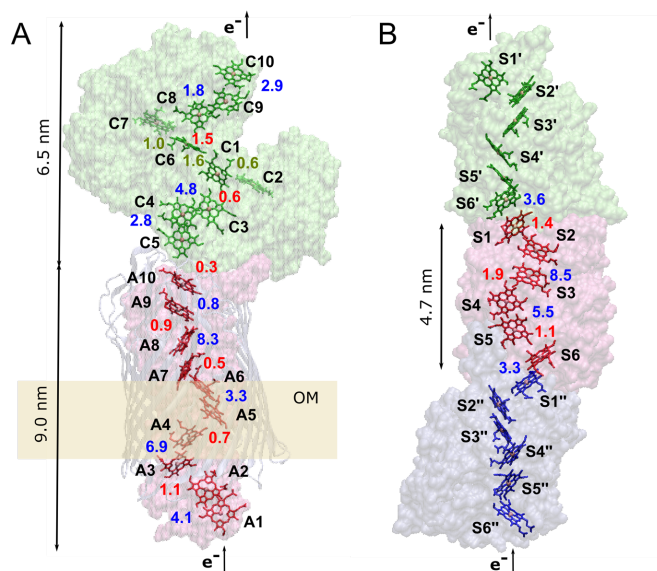
Figure 1. Crystal structures of Multi-heme proteins. (A) MtrCAB complex from *Shewanella baltica* OS185 (PDB ID 6R2Q) and a section of the OmcS polymer containing three repeat units from *Geobacter sulfurreducens* (PDB ID 6EFB). In (A), MtrA, MtrB and MtrC are shown in shaded red, gray and green, respectively and heme cofactors are highlighted in stick representation. Hemes of MtrA are labeled A1-10 and hemes of MtrC C1-C10. The position of the outer bacterial membrane (OM) relative to MtrAB is depicted by a yellow bar. In (B), the three OmcS repeat units are shaded in blue, red and green and hemes are labeled S1''-S6'', S1-S6 and S1'-S6', respectively. The heme-heme electronic couplings (in units of meV) are color-coded by heme packing motif: blue, stacked; red, T-shaped; green, co-planar.

MtrCAB is an outer-membrane (OM) spanning protein complex comprised of MtrA, MtrB and MtrC, see Figure 1A [6]. The 10-heme protein MtrA spans the OM and is insulated from the lipid bilayer by embedding within a beta-barrel formed by MtrB. The MtrAB complex binds the 10-heme protein MtrC non-covalently on the extracellular side. This particular arrangement gives rise to a continuous 18-heme transmembrane ET pathway that runs perpendicular to the membrane, from heme A1 of MtrA to heme C10 of MtrC. The remaining 2 hemes in MtrC, C2 and C7, allow for branching of the ET path in lateral directions to adjacent MtrCAB complexes along the membrane. The protein polymer of *Geobacter* has a simpler structure; it is formed through polymerization of the hexa-heme cytochrome OmcS which gives rise to a continuous ET pathway with a repeat unit of 6 hemes, see Figure 1B [5]. Interestingly, in both MtrA and OmcS the hemes are arranged in an alternating shifted-stacked (S) and T-shaped (T) motif which brings the edges of adjacent hemes in or close to van-der-Waals contact. In MtrC a third, co-planar (C) motif is found.

Here we focus on electron transfer (ET) through these protein complexes in aqueous solution, where chemical species rather than electrodes serve as external electron donor on one terminus of the protein complex and as electron acceptor on the other, much like in the natural respiratory process. Previous theoretical[7-9] and spectroscopic work[10] have established that under these conditions ET through multi-heme proteins occurs via heme-to-heme hopping – the electronic coupling between the hemes is too small compared to reorganization energy to support other mechanisms such as flickering resonance or band-like transport [8, 11]. We note in passing that the mechanism for electron transport (ETp), i.e., conductance of multi-heme proteins, as probed e.g. by scanning tunneling microscopy[12-13], monolayer junctions[14] or direct current measurements[5], may differ from hopping and is expected to depend on details of the electrode-protein interface and degree of protein solvation.

In the following we present the key parameters governing the heme-heme ET (Marcus) rates, electronic coupling, reorganization free energy, and driving force before discussing the predicted electron flow. The electronic couplings between adjacent Fe^{2+}-Fe^{3+}-heme pairs are obtained from density functional theory (DFT) calculations using the projector operator-based diabatization (POD) method as described and validated against high-level ab-initio calculations in Ref [15], see SI for details. The electronic couplings in the two protein complexes are similar though slightly higher on average in OmcS. As expected, the stacked heme pairs exhibit the largest couplings (1-9 meV, indicated in blue in Fig.1) followed by the T-shaped and co-planar pairs (0.3-2 meV, indicated in red and green, respectively).

The strength of the electronic connection across the protein-protein interfaces is of particular interest - *a priori* one would expect this to be the weakest link in the ET chain. Not so in OmcS. Either of the two interfaces is formed by a tightly stacked heme pair (3.9 Å edge-to-edge for S1''-S6 and S1-S6') with relatively high couplings (3.3 meV and 3.6 meV). By contrast, the adjacent hemes crossing the MtrAB-MtrC interface, A10-C5, are further apart (8.0 Å edge-to-edge) resulting in a significantly smaller coupling strength (0.3 meV). Yet, this value is an order of magnitude higher than what one would expect from simple through-space exponential distance decay between the heme edges[7]. Our DFT calculations reveal that when all side chains of hemes A10 and C5 (methyl, propionates, Cys linkages) except Cys linkage 306 of heme C5 are included in the model, the coupling increases from 0.01 meV to 0.1 meV, with respect to the unsubstituted heme (=porphin) ring. Cys linkage 306 inserts in the space between heme A10 and C5 and increases electronic coupling further to the final value of 0.3 meV (see Figure 2). Evidently, the heme side chains augment the tails of the redox-active Fe-heme d orbitals leading to an increase in orbital overlap and electronic coupling. The corresponding increase in ET rate is almost 1000-fold. Similar coupling enhancements were seen before for intra-protein ET steps in MtrC[9], MtrF[9] and STC[16].

Our present results show that the same mechanism is used to accelerate inter-protein tunneling between multi-heme proteins.
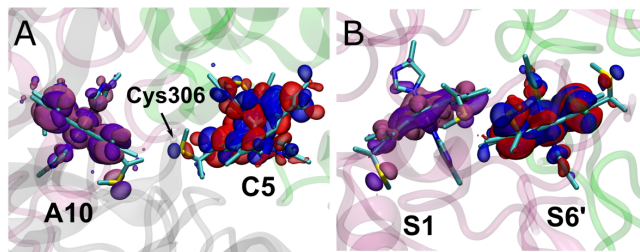

Figure 2. Protein-protein interface in MtrCAB (A) and the OmcS polymer (B). The backbone of the proteins is depicted in cartoon representation using the same color code as Figure 1. The adjacent hemes crossing the protein interface are highlighted in stick representation and isosurfaces of the Fe-heme frontier orbital pairs mediating the electron transfer are superimposed.

Reorganization free energy in bis-His coordinated cytochromes is predominantly due to the outer-sphere contribution, i.e. protein and solvent[8]. In previous work we have shown that this contribution can be well described by the Marcus continuum formula in combination with a static dielectric constant of the medium that is a linear function of the solvent-accessible surface area (SASA) of the electron donating and electron accepting heme groups[9], see SI for details. We find that reorganization free energy is smaller on average for OmcS (0.71 eV) than for MtrCAB (0.82 eV) due to less solvent exposure of the hemes. The third ET parameter, driving force or heme reductions potential difference, is obtained from (linearized) Poisson-Boltzmann continuum electrostatics calculations[17], see SI for details. The computed potentials for MtrCAB fall within a range of 0.3V, reasonably close to the 0.4V window obtained from cyclic voltammetry[3].

The resultant Marcus heme-heme ET rates are used to solve a chemical master equation for the steady-state electron flux through the two protein complexes, J_{max}[7-9]. To ensure a fair comparison, we consider the 18-heme ET path in MtrCAB and a 18-heme OmcS trimer as shown in Figure 1B. Both ET paths not only feature the same number of hemes but also span a very similar distance, 139 Å and 134 Å measured Fe to Fe from heme A1 to C10 in MtrCAB and heme S6" to heme S1' in OmcS. As we are interested in the intrinsic, protein-limited electron flow rather than interfacial effects with external donors and acceptors, we assume that electron input and output is much faster than any ET steps within the protein complex.

The results are summarized in Figure 3. We obtain an electron export flux of 2×10^6 s^{-1} and 2×10^5 s^{-1} for the two separate proteins MtrC and MtrAB, respectively. The value reported here for MtrC from *Shewanella baltica* is about an order of magnitude larger than the previously reported value for MtrC from *Shewanella oneidensis*. In the latter ET was limited by the relatively large up-hill driving force for the ET step C4→C3. Present calculations

predict that this step is close to thermoneutral and no longer flux-limiting in the MtrC protein from *Shewanella baltica*.
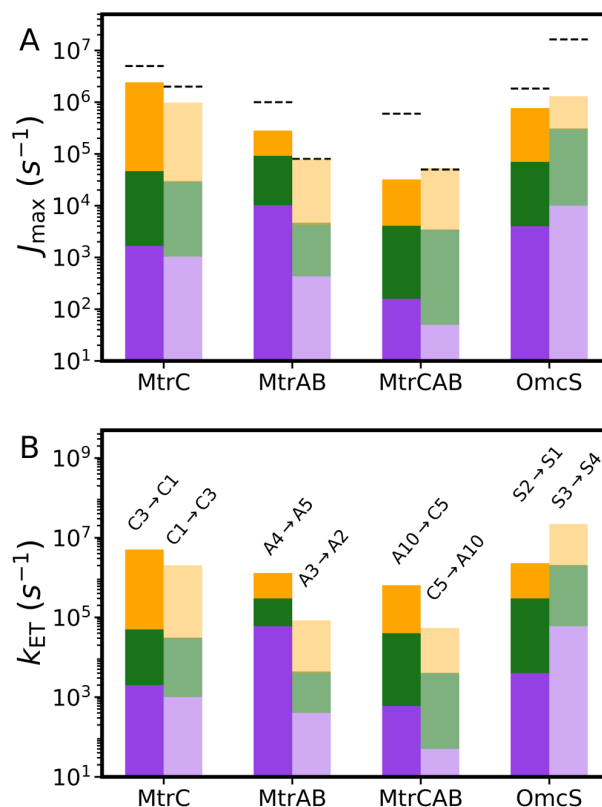

Figure 3. Kinetics of electron transfer through multi-heme protein complexes. (A) Intrinsic, i.e. protein-limited steady-state electron flux J_{max} and (B) slowest heme-heme ET step in the respective flow direction. Filled bars are for the directions A1→C10 for MtrCAB (18 hemes), A1→A10 for MtrAB (10 hemes), C5→C10 for MtrC (8 hemes) and S6"→S1' for OmcS trimer (18 hemes), shaded bars are for the reverse directions. The flux and slowest ET rates shown in purple are based on electronic couplings obtained for a heme model with all side chains replaced by hydrogens. The increase in flux and slowest ET rate due to inclusion of all heme side chains in the coupling calculation, except the Cys linkages that insert in the space between adjacent heme groups, is shown in green. The effect of the latter Cys linkages is shown in orange. In (A), the slowest ET step is reproduced from panel (B) and shown in dashed lines.

Considering the full MtrCAB complex, we obtain a flux that is significantly smaller than for MtrC and MtrAB, 3×10^4 s^{-1} (heme A1→C10), suggesting that the MtrAB-MtrC protein interface limits the export flux. It turns out there are two flux-limiting ET steps: as expected, the ET step crossing the interface between MtrAB and MtrC, heme A10→C5, as well as the intra-protein step A4→A5 in MtrA. Both steps are slow due to a combination of small electronic coupling (see discussion above for A10→C5) and a relatively large reorganization free energy. The electron flux through the OmcS trimer is a factor of about 30 higher than in MtrCAB (7×10^5 s^{-1} in the S6"→S1' and 1×10^6 s^{-1} in the S1'→S6" directions) and there is no clearly flux limiting step. In both protein complexes electron flow is remarkably reversible: import and

export flux differ by less than a factor of two. In Figure 3 we also indicate the fluxes and slowest ET rates when the electronic coupling enhancement due to heme side chains are excluded (bars in purple). For both protein complexes this leads to a dramatic decrease in the flux by about 2 orders of magnitude.

Before we compare our results to experiment some clarification with regard to the calculations is in order. The electron transfer parameters used for the calculation of ET rates and fluxes largely rely on static protein structures and do not explicitly include thermal protein fluctuations. This should not be a major problem for MtrCAB because thermal corrections for electronic coupling and estimation of reorganization energy from solvent accessibility are based on explicit MD data obtained previously for very similar multi-heme cytochromes from *Shewanella* including MtrC, MtrF, NrfB and STC.[9] OmcS on the other hand has a much higher percentage of relatively unstructured turns and coils[5] which might give rise to more pronounced dynamical effects on electron transfer than observed for the multi-heme proteins of *Shewanella*. Future explicit molecular dynamics simulation on OmcS may shine light on this issue.

There are several experimental findings that lend support to our results. Firstly, the ET rate constant for a T-shaped heme pair was recently determined in the tetraheme cytochrome STC using transient absorption spectroscopy, 8.7×10^7 s^{-1} (heme 4$\rightarrow$3)[10]. This falls in the range of computed values for T-shaped heme pairs in MtrCAB and OmcS, 2×10^6-1×10^8 s^{-1}, after normalizing the rate to the same driving force as in STC. Secondly, the electron flux through MtrCAB adsorbed on an Fe(III)-oxide nanoparticle was determined to be 1.0×10^4 s^{-1} [18], consistent with computations (3×10^4 s^{-1}). Our predicted value is expected to be larger than the experimental estimate because the latter was shown to be limited by the interfacial ET step to the oxide, not the protein. Thirdly, the thermal activation free energy for the Mtr pathway-dependent conduction across *Shewanella oneidensis* MR1 was determined to be $\Delta A^{\neq}$=0.29 eV.[19] This value can be interpreted as an upper bound to the activation free energy for ET across MtrCAB. It compares favorably with our computed activation free energy obtained from an Arrhenius plot of the temperature-dependence of J_{max}, $\Delta A^{\neq}$ = 0.28 eV. Fourth, the conductivity of OmcS filaments was recently reported to be about 35 mS cm^{-1} [5], a factor of about 15 higher than the value we determine from the STM data for MtrC[12] (2.3 mS cm^{-1} assuming an electrode separation of 6.5 nm and the same cross section area as in OmcS). Although we do not know if the conductivity is limited by the protein or the contacts in either measurements, we notice that the difference in conductivity is similar to the difference in the computed protein-limited electron flux.

To summarize, we have computed the intrinsic electron flow along the 18-heme ET path formed by MtrCAB and a OmcS trimer. We find that the latter permits a higher intrinsic electron flow because the hemes are more tightly packed, especially at protein interfaces, but also due to a more uniform reduction of solvent exposure of the heme chain resulting in smaller ET activation barriers. Nonetheless, electron flow in MtrCAB is surprisingly high given the unfavorably large heme edge-to-edge distance across the MtrA-MtrC protein interface. We found that this ET step is strongly accelerated by the side chains of the heme rings. Such tunneling enhancements could ensure that electrons do not accumulate in the periplasm of the bacterial cells. Moreover, the alternating stacked/T-shaped heme packing seen in both MtrCAB and OmcS may be evolutionarily convergent in terms of efficient long-range electron transfer.

Finally, we note that the higher ET efficiency of OmcS compared to MtrCAB may not necessarily lead to greater in-vivo microbial electron export rates. The latter are a function of a large number of parameters including the bacterial central metabolism, and they are in fact found to be comparable for both bacteria[20,21]. Though we expect our findings have important implications for the use and design of native and bioinspired heme-nanowires in future bionanotechnological applications.

ASSOCIATED CONTENT

AUTHOR INFORMATION

Corresponding Author
*j.blumberger@ucl.ac.uk

ACKNOWLEDGMENT

Supporting Information Available: The calculation of ET parameters, ET rate constants and electron fluxes are summarized in the Supporting Information.

REFERENCES

(1)   Myers, C. R.; Nealson, K. H. Bacterial manganese reduction and growth with manganese oxide as the sole electron acceptor. *Science* **1988,** *240*, 1319-1321.

(2)   Chong, G. W.; Karbelkar, A. A.; El-Naggar, M. Y. Nature's conductors: what can microbial multi-heme cytochromes teach us about electron transport and biological energy conversion? *Curr. Opin. Chem. Biol.* **2018,** *47*, 7-17.

(3)   Hartshorne, R. S.; Reardon, C. L.; Ross, D.; Nuester, J.; Clarke, T. A.; Gates, A. J.; Mills, P. C.; Fredrickson, J. K.; Zachara, J. M.; Shi, L.; *et al.* Characterization of an extracellular conduit between bacteria and the extracellular environment. *Proc. Natl. Acad. Sci. USA* **2009,** *106*, 22169-22174.

(4)   Subramanian, P.; Pirbadian, S.; El-Naggar, M. Y.; Jensen, G. J. Ultrastructure of Shewanella oneidensis MR-1 nanowires revealed by electron cryotomography. *Proc. Nat. Acad. Sci. USA* **2018,** *115*, E3246-E3255.

(5)   Wang, F.; Gu, Y.; O'Brien, J. P.; Yi, S. M.; Yalcin, S. E.; Srikanth, V.; Shen, C.; Vu, D.; Ing, N. L.; Hochbaum, A. I.; *et al.* Structure of microbial nanowires reveals stacked hemes that transport electrons over micrometers. *Cell* **2019,** *177*, 361-369.

(6)   Edwards, M. J.; White, G. F.; Butt, J. N.; Richardson, D. J.; Clarke, T. A. The crystal structure of a biological insulated transmembrane molecular wire. *Cell* **2020,** *181*, 665-673.

(7)   Breuer, M.; Rosso, K. M.; Blumberger, J. Electron flow in multi-heme bacterial cytochromes is a balancing act between heme electronic interaction and redox potentials. *Proc. Nat. Acad. Sci. USA* **2014,** *111*, 611-616.

(8)   Blumberger, J. Recent advances in the theory and molecular simulation of biological electron transfer reactions. *Chem. Rev.* **2015,** *115*, 11191-11238.

(9)   Jiang, X.; Burger, B.; Gajdos, F.; Bortolotti, C.; Futera, Z.; Breuer, M.; Blumberger, J. Kinetics of trifurcated electron flow in the decaheme bacterial proteins MtrC and MtrF. *Proc. Nat. Acad. Sci. USA* **2019,** *116*, 3425-3430.

(10)   Wonderen, J. H. v.; Hall, C. R.; Jiang, X.; Adamczyk, K.; Carof, A.; Heisler, I.; Piper, S. E. H.; Clarke, T. A.; Watmough, N. J.; Sazanovich, I. V.; *et al.* Ultra-fast light-driven electron transfer in a Ru(II)tris(bipyridine)-labelled multiheme cytochrome. *J. Am. Chem. Soc.* **2019,** *141*, 15190-15200.

(11)   Polizzi, N. F.; Skourtis, S. S.; Beratan, D. N. Physical constraints on charge transport through bacterial nanowires. *Faraday Discuss.* **2012,** *155*, 43-62.

(12)   Wigginton, N. S.; Rosso, K. M.; Lower, B. H.; Shi, L.; Hochella, M. F. J. Electron tunneling properties of outer-membrane decaheme cytochromes from Shewanella oneidensis. *Geochim. Cosmochim. Acta* **2007,** *71*, 543-555.

(13)   Byun, H. S.; Pirbadian, S.; Nakano, A.; Shi, L.; El-Naggar, M. Y. Kinetic Monte Carlo simulations and molecular conductance measurements of the bacterial decaheme cytochrome MtrF. *ChemElectroChem* **2014,** *1*, 1932-1939.

(14)   Garg, K.; Ghosh, M.; Eliash, T.; Wonderen, J. H. v.; Butt, J. N.; Shi, L.; Jiang, X.; Futera, Z.; Blumberger, J.; Pecht, I.; *et al.* Direct evidence for heme-assisted solid-state electronic conduction in multi-heme c-type cytochromes. *Chem. Sci.* **2018,** *9*, 7304-7310.

(15)   Futera, Z.; Blumberger, J. Electronic couplings for charge transfer across molecule/metal and molecule/semiconductor interfaces: performance of the projector operator-based diabatization approach. *J. Phys. Chem. C* **2017,** *121*, 19677-19689.

(16)   Jiang, X.; Futera, Z.; Ali, M. E.; Gajdos, F.; Rudorff, G. F. v.; Carof, A.; Breuer, M.; Blumberger, J. Cysteine linkages accelerate electron flow through tetra-heme protein STC. *J. Am. Chem. Soc.* **2017,** *139*, 17237-17240.

(17)   Li, L.; Li, C.; Sarkar, S.; Zhang, J.; Witham, S.; Zhang, Z.; Wang, L.; Smith, N.; Petukh, M.; Alexov, E. DelPhi: a comprehensive suite for DelPhi software and associated resources. *BMC Biophys.* **2012,** *5*, 9.

(18)   White, G. F.; Shi, Z.; Shi, L.; Z. Wang; Dohnalkova, A. C.; Marshall, M. J.; Fredrickson, J. K.; Zachara, J. M.; Butt, J. N.; Richardson, D. J.; *et al.* Rapid electron exchange between surface-exposed bacterial cytochromes and Fe(III) minerals. *Proc. Nat. Acad. Sci. USA* **2013,** *110*, 6346-6351.

(19)   Xu, S.; Barrozo, A.; Tender, L. M.; Krylov, A. I.; El-Naggar, M. Y. Multiheme cytochrome mediated redox conduction through Shewanella oneidensis MR-1 cells. *J. Am. Chem. Soc.* **2018,** *140*, 10085-10089.

(20)   Jiang, X. C; Hu, J. S.; Petersen, E. R.; Fitzgerald, L. A.; Jackan, C. S.; Lieber, A. M.; Ringeisen, B. R.; Lieber, C. M.; Biffinger, J. C. Probing single- to multi-cell level charge transport in *Geobacter sulfurreducens* DL-1. *Nat. Comm.* **2013,** *4*, 2751.

(21)   Gross, B. J.; El-Naggar, M. Y. A combined elec-trochemical and optical trapping platform for measuring single cell respiration rates at electrode interfaces. *Rev. Sci. Instrum.* **2015***, 86,* 064301.